Journal of Hazardous Materials 472 (2024) 134548

Contents lists available at ScienceDirect

Journal of Hazardous Materials

journal homepage: www.elsevier.com/locate/jhazmat

Simultaneous Cu(II)-EDTA decomplexation and Cu(II) recovery using integrated contact-electro-catalysis and capacitive deionization from electroplating wastewater

Xiaoyan Shen [a], Shiyong Wang [a], Lin Zhao [b], Haoran Song [d], Wei Li [a], Changping Li [a], Sihao Lv [a], Gang Wang [a,c,*,1]

[a] School of Environment and Civil Engineering, Research Center for Eco-Environmental Engineering, Dongguan University of Technology, Dongguan 523106, Guangdong, China
[b] College of Chemical Engineering, Beijing University of Chemical Technology, Beijing 100029, China
[c] Guangdong Provincial Key Laboratory of Intelligent Disaster Prevention and Emergency Technologies for Urban Lifeline Engineering, Dongguan 523106, Guangdong, China
[d] Faculty of Environmental Science and Engineering, Kunming University of Science and Technology, Kunming 650500, Yunnan, China

HIGHLIGHTS

- The reactive oxygen species were generated in CEC without extra oxidants.
- FEP as dielectric powders could effectively degrade Cu(II)-EDTA in CEC.
- CEC coupled CDI could degrade Cu(II)-EDTA and directly capture Cu^{2+}.
- The decomplexation of Cu(II)-EDTA in CEC was dominated by decarboxylation.

GRAPHICAL ABSTRACT

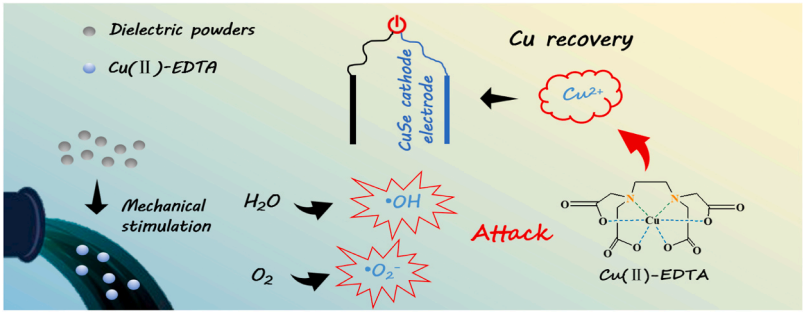

ARTICLE INFO

Keywords:
Heavy metal complexes
Decomplexation
Contact-electro-catalysis
Cu recovery

ABSTRACT

The complex of heavy metals and organic acids leads to high difficulty in heavy metals separation by traditional technologies. Meanwhile, alkaline precipitation commonly used in industry causes the great consumption of resources and extra pollution. Herein, the effective decomplexation of Cu(II)-EDTA and synchronous recycling of Cu^{2+} were realized by contact-electro-catalysis (CEC) coupled with capacitive deionization (CDI) innovatively. In particular, fluorinated ethylene propylene (FEP) as dielectric powders could generate reactive oxygen species under ultrasonic stimulation, realizing continuous deaminization and decarboxylation of Cu(II)-EDTA and accelerating the totally breakage of Cu-O and Cu-N bonds. Additionally, the degradation pathway and intermediates evolution of Cu(II)-EDTA were investigated using various characterization methods. It was confirmed that decarboxylation predominantly governed the degradation process of Cu(II)-EDTA in CEC. During the course of treatment, the degradation ratio of Cu(II)-EDTA reached 86.4 % within 150 min. Impressively, this

* Corresponding author at: School of Environment and Civil Engineering, Research Center for Eco-Environmental Engineering, Dongguan University of Technology, Dongguan 523106, Guangdong, China.
E-mail address: wghy1979@163.com (G. Wang).
[1] orcid.org/0000-0002-3185-1268.

https://doi.org/10.1016/j.jhazmat.2024.134548
Received 25 January 2024; Received in revised form 14 April 2024; Accepted 3 May 2024
Available online 7 May 2024

strategy had satisfactory applicability to other metal combinations and excellent cycle stability. Subsequently, the released Cu ions were captured by CuSe cathode electrode through CDI. This research elucidated the degradation mechanism of persistent organic pollutant during CEC, and provided a novel approach for efficiently treating industrial wastewater containing metal complexes and advancing the exploitation and utilization of new technologies for metal recovery.

1. Introduction

The increasingly severe contamination of toxic heavy metals and the depletion of copper (Cu) resources have posed a formidable challenge in addressing heavy metal pollution treatment and Cu^{2+} recycling [1,2]. On account of its strong affinity for amino, carboxyl and other functional groups [3], Cu^{2+} is easy to bond with organic ligands in the wastewater to produce metal complex like ethylenediaminetetraacetic acid-chelated copper [Cu(II)-EDTA], which have stronger toxicity and faster diffusion rate [4,5]. Some industrial enterprises, such as mining, metallurgic and electroplating, would also generate and discharge significant quantities of metal wastewater containing Cu(II)-EDTA, thereby inevitably causing environmental harm [6–8]. The effective removal of Cu(II)-EDTA using traditional wastewater treatment methods such as ion exchange, adsorption, and precipitation is challenging [9–11]. Therefore, it is of paramount importance to develop a sewage treatment method that can effectively disrupt the metal-organic bond of Cu(II)-EDTA and facilitate the recycling of valuable metal resources.

In recent years, advanced oxidation processes (AOPs) have been extensively used for the treatment of metal complexes wastewater because of the strong oxidation ability of generating hydroxyl radical (•OH) [12], which can effectively break down metal-organic bonds of metal complexes and facilitate the release of metal ions after decomplexation, such as persulfate oxidation [13,14], photochemical oxidation [15–17], ozonation [18,19], Fenton oxidation [20,21]. However, there may be some defects, such as poor oxidization [22], the need for high energy consumption or a large number of chemical reagents, the need to achieve a better treatment effect at a lower pH [23], the degradation effect falls short of expectations and other problems [24]. Furthermore, these AOPs generally require additional precipitation to remove metal ions after decomplexation, which undoubtedly add the cost, also easily cause secondary pollution, increasing the burden on the environment.

As an innovative strategy for generating reactive oxygen species (ROS) and treating refractory organic pollutants, contact-electro-catalysis (CEC) is at the forefront of mechanochemistry, contact-electrification and catalysis. It has been proved that it had the efficient degradation capability to challenge organic pollutants including methyl orange and crystal violet [25,26]. The electrons that drive the exchange in the contact-electrification can be used for CEC [27], where the mechanical stimulation creates cavitation bubbles, and the electron transfer during the generation and rupture phenomena of cavitation bubbles occurring on the surface of dielectric powder generates surface electrostatic charges. These electrostatic charges are transferred to generate ROS, which react with refractory organic compounds to achieve the degradation of organic pollutants [28]. At the same time, the capacitive deionization (CDI) has witnessed rapid development in the past decade, offering a novel approach to desalting [29]. Compared with the traditional desalination method, CDI boasts several advantages including superior desalting efficiency [30], simplified desorption operation, reduced energy consumption and minimized secondary pollution [31], and enables to selectively capture Cu^{2+} in wastewater effectively [32].

In this research, an all-electrified approach which coupled CEC and CDI for the first time was reported to enable the effective degradation of Cu(II)-EDTA and coinstantaneous recovery of Cu^{2+}. Specifically, fluorinated ethylene propylene (FEP) as dielectric powders could produce ROS under ultrasonic stimulation and achieve effective degradation of Cu(II)-EDTA. The free Cu^{2+} after decomplexation would be electro-adsorbed by the CuSe cathode electrode in CDI. In the process of Cu^{2+} adsorption by CuSe, Cu^{2+} were stored in the electrode as cuprous selenide (Cu_2Se). In addition, the existence of hydroxyl radical (•OH) and superoxide radical ($\bullet O_2^-$) was verified by electron paramagnetic resonance (EPR), and the energy barrier of electron exchange between FEP and water/O_2 under reaction conditions was evaluated by DFT to discuss the internal mechanism of CEC degradation of organic pollutants. Meanwhile, the degradation pathway and intermediates evolution of Cu(II)-EDTA were researched by high performance liquid chromatography mass spectrometry (HPLC-MS). Overall, this study provided new inspiration for the decomplexation and recovery of Cu(II)-EDTA, and may also stimulate further explorations of chemical processes induced by CEC.

2. Materials and methods

2.1. Contact-electro-catalysis experiments

50 mg of FEP was added to a 50 mL solution of Cu(II)-EDTA with a concentration of 0.1 mmol/L. FEP particles were fully in contact with the solution through magnetic agitation. The solution, which consists of FEP and Cu(II)-EDTA, was subsequently placed in an ultrasonic cleaner (KQ-200VDE) for 150 min. A certain volume of solution was extracted from the original solution at intervals and the concentration of Cu(II)-EDTA was determined by high performance liquid chromatography (HPLC).

2.2. CDI experiments

80 wt% CuSe, 10 wt% carbon black, 10 wt% compound of polyvinyl butyric aldehyde (PVB) and polyvinylpyridone (PVP) were mixed into a uniform slurry and coated on graphite paper (2×3 cm^2) and dried at 80 ℃ overnight. With CuSe as the cathodes and platinum sheet electrode as the anodes, a two-electrode system was formed. 50 mL of aqueous solution after CEC was added in electrode system, and the required voltage was provided by electrochemical workstation (CHI 660E) for CDI experiments. During the 4-hour electroadsorption process, a certain volume of solution was extracted from the original solution at intervals, and the concentration of Cu^{2+} was measured by inductively-coupled plasma optical emission spectrometer (ICP-OES).

2.3. Analytical methods

The morphology and structure of the samples were observed by field emission scanning electron microscopy (FE-SEM, FEI Sirion200). The elements contained of the sample was analyzed by Energy Dispersive X-Ray analysis (EDX, FEI Sirion200) The structure composition of the samples was explored by X-ray diffractometer (XRD, Bruker D8). FT-IR (FRONTIER) was applied to characterize the functional structures of samples. The composition of the sample was analyzed by X-ray photoelectron spectroscopy (XPS, ESCALAB XI). The Raman spectrum was measured on a Raman spectrometer (XPLORA PLUS). The concentrations of Cu(II)-EDTA was measured on a high-performance liquid chromatography (HPLC, Agilent 1260 Infinity, USA) instrument. ROS including hydroxyl radical (•OH) and superoxide radicals ($\bullet O_2^-$) were determined using 5,5-dimethyl-1-pyrroline-N-oxide (DMPO) as the spin-trapping agent by electron paramagnetic resonance (EPR, Bruker

BRUKER A200). The quantitative detections of H_2O_2 was implemented using a UV–vis spectrophotometer (L6, Yidian, Shanghai). The intermediate generation during the decomplexation of Cu(II)-EDTA was identified by high performance liquid chromatography-mass spectrometry (HPLC-MS, U3000RSLC-Q Exactive Focus, Thermo Fisher Scientific, USA). The CDI experiments was conducted by an electrochemical workstation (CHI 660E Chenhua, Shanghai). Inductively-coupled plasma optical emission spectrometer (ICP-OES, PerkinElmer Optima 8000) was used to quantify the concentrations of Cu^{2+} in solution. The energy barrier of electron exchange in the sample was calculated through density functional theory (DFT).

3. Results and discussion

3.1. Investigation of properties and characteristics of dielectric powders

The experimental apparatus for Cu(II)-EDTA decomplexation was exhibited in Fig. 1a. Previous studies have shown that dielectric materials could be energized in contact with water to drive catalytic reactions and synthesize H_2O_2 [33]. Therefore, different dielectric powders, such as FEP, $BaTiO_3$, polyvinylidene fluoride (PVDF) and polytetrafluoroethylene (PTFE), were used to study the relationship between dielectric powders and degradation efficiency of Cu(II)-EDTA. The dielectric material FEP, as depicted in Fig. 1b-c, exhibited a remarkable ability to decomplexed 86.4 % of Cu(II)-EDTA during the CEC process within a time frame of 150 min, with a reaction rate constant of 0.01543 min^{-1}, but the degradation efficiency of $BaTiO_3$, PVDF and PTFE for Cu (II)-EDTA was 42.0 %, 17.7 % and 27.2 %, and the reaction rate constant was only 0.00427, 0.00167 and 0.00226 min^{-1}, respectively. The quantity of hydrogen peroxide (H_2O_2) generated during the CEC process in the solution was measured without the introduction of any contaminants (Fig. S1). It could be observed that under the continuous stimulation of ultrasonic, the concentration of H_2O_2 continued to accumulate, and the concentration of H_2O_2 in the FEP solution was markedly higher than that added with other dielectric powders, which indirectly verified the generation of ROS in CEC process, such as •OH, and underscored the correlation between the catalytic performance and the properties of dielectric material.

The physicochemical properties of FEP were investigated using various characterization methods before and after ultrasound to clarify the role of dielectric powder in the catalytic reaction. Scanning electron microscopy (SEM) and energy dispersive X-ray analysis (EDS) (Figs. S2–3) indicated that the morphology and element distribution of FEP powder after ultrasound were consistent with those before the

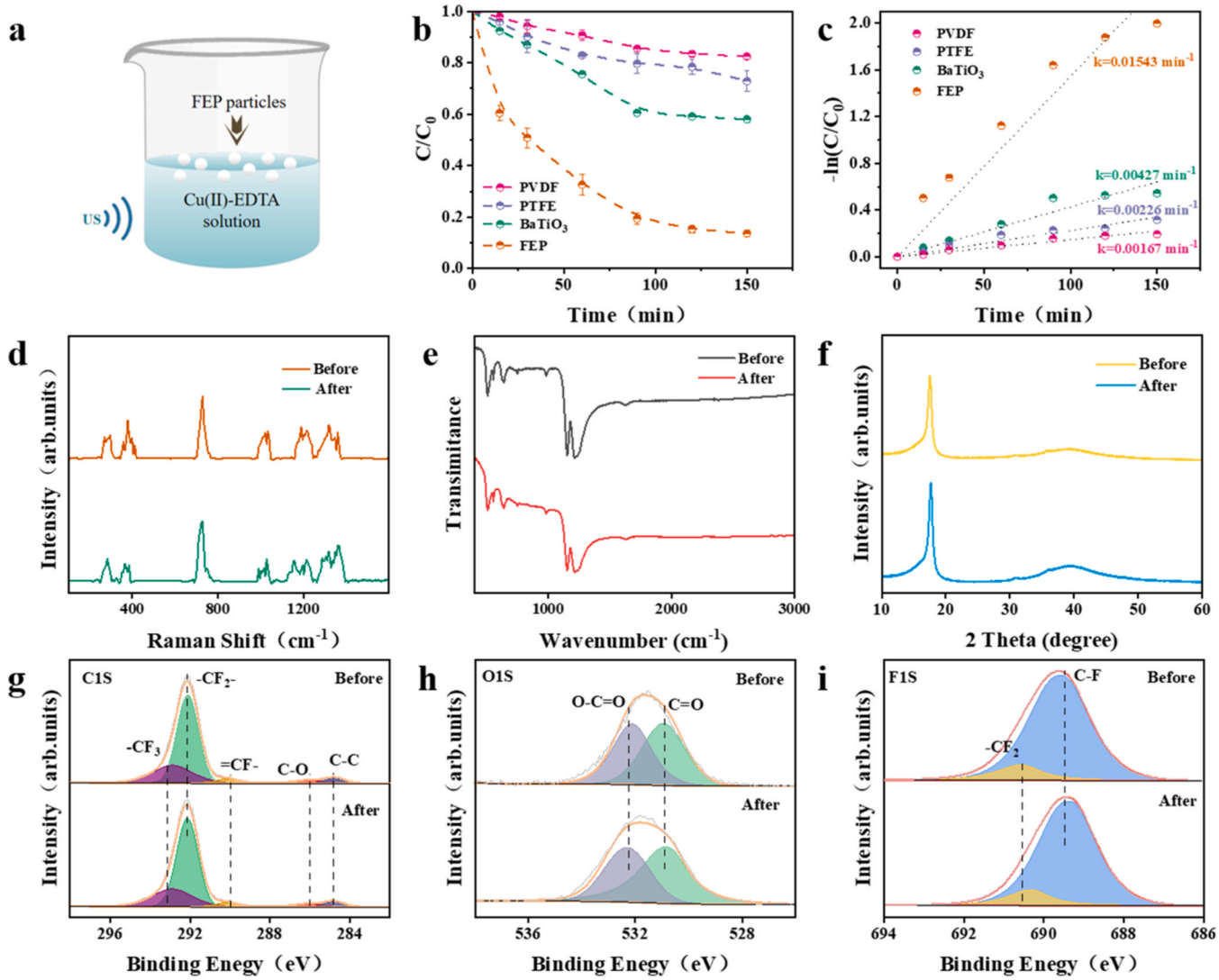

Fig. 1. (a) Schematic representation about CEC experimental setup. (b) Plots of Cu (II)-EDTA reduction of FEP, PVDF, PTFE and $BaTiO_3$ during CEC process, and (c) $-\ln(C/C_0)$ versus time. (d) Raman spectra, (e) Fourier transform infrared spectra and (f) XRD of FEP before and after reaction. (g) C1s, (h) F1s, and (i)O1s XPS spectra of FEP before and after reaction.

catalytic reaction. The skeleton vibration mode was uniform through Raman spectrometer as well (Fig. 1d). In Fourier transform infrared (FT-IR) and X-ray diffractometry (XRD) analysis results (Fig. 1e-f), FEP particles were also stable after the catalytic reaction. From X-ray photoelectron spectroscopy (XPS) spectrums of C1s, F1s and O1s of FEP powders (Fig. 1g-i), it could be found that the original peaks did not dissimilate and no new peaks were generated after the reaction, which confirmed the chemical stability of FEP particles during CEC and ruled out the possibility of adsorption. These analyses illustrate that FEP functioned as a catalyst in the decomplexation process of Cu(II)-EDTA. In the meantime, the results of each characterization were consistent with previous studies on FEP [27,33].

3.2. Cu(II) -EDTA decomplexation performance

As displayed in Fig. S4, under the action of ultrasound and FEP, the concentration of Cu(II)-EDTA in the solution decreased by 86.4 % within 150 min, which has certain advantages over traditional ozone oxidation. In contrast, the effect of Cu(II)-EDTA degraded with ultrasonic alone could be ignored. In the CEC process, the growth and rupture of cavitation bubbles play a crucial role in achieving effective degradation of refractory organic pollutants, while the frequency and power of ultrasonic determine both the quantity and size of cavitation bubbles. Therefore, the decomplexation of Cu(II)-EDTA were compared under different ultrasonic frequency (45–100 KHz) and different ultrasonic power (80–200 W). As shown in Fig. 2a-b, Cu(II)-EDTA showed a high degradation rate of nearly 90% at the ultrasonic frequency of 45 KHz with the reaction rate constant of 0.01543 min^{-1}. However, the degradation efficiencies were significantly worse at 80 and 100 KHz, which were 47.8 % and 16.5 %, and the reaction rate constants were 0.00512 and 0.00122 min^{-1}, respectively. When the ultrasonic frequency was high, the oscillation frequency would be accelerated. But in fact, the increase in oscillation frequency would cause a corresponding decrease in ultrasonic wavelength, leading to a significant rise in attenuation during ultrasonic propagation. This phenomenon hinders the efficient utilization of ultrasonic energy. The decomplexation efficiencies of Cu (II)-EDTA under various ultrasonic power of 45 KHz were plotted in Fig. 2c-d. The decomplexation rate of Cu(II)-EDTA went up with the augmentation of ultrasonic power, with a concurrent increase in the reaction rate constant. It is obvious that the enhancement of the ultrasonic power would augment the quantity of cavitation bubbles and the input energy, so as to promote the degradation of organic pollutant.

The decomplexation of Cu(II)-EDTA with different dosages of FEP particles was investigated. Fig. 2e indicated that the degradation ratio of

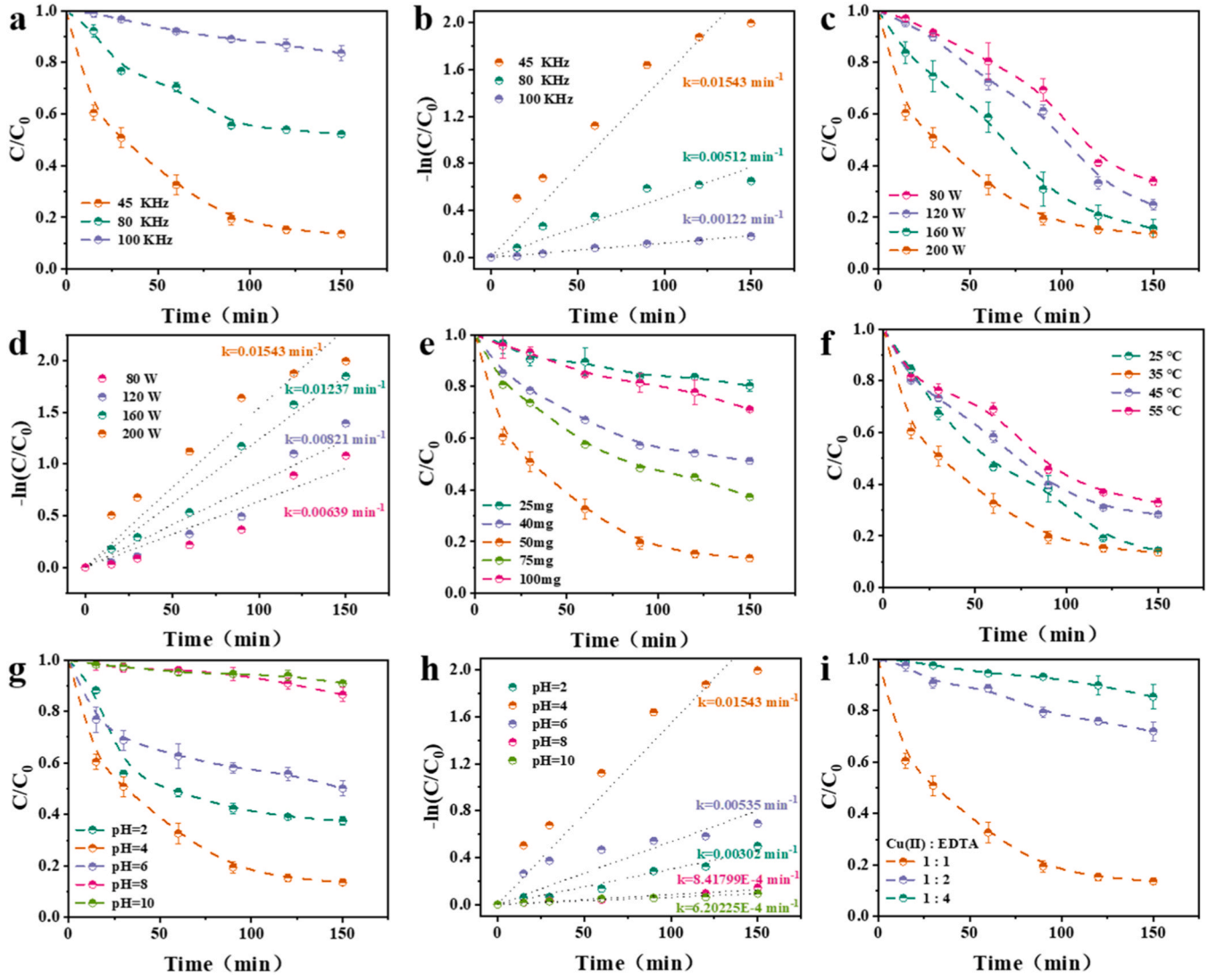

Fig. 2. (a) Plots of Cu(II)-EDTA decomplexation during CEC at various ultrasonic frequencies and (b) $-\ln(C/C_0)$ versus time. (c) Plots of Cu(II)-EDTA decomplexation during CEC at various ultrasonic power and (d) $-\ln(C/C_0)$ versus time. Plots of Cu(II)-EDTA decomplexation during CEC at various (e) dosage of FEP particles, (f) temperature, (g) pH and (h) $-\ln(C/C_0)$ versus time, (i) molar ratios of Cu and EDTA versus time.

Cu(II)-EDTA initially increased and then decreased along with the continuous addition of FEP powder. There was no doubt that FEP could be fully in contact with the solution due to the increase in dosage, but excessive electrons would accumulate on the surface of dielectric powder and lead to the formation of a high electric field [34], thus inhibiting the generation of ROS and affecting the effect of Cu(II)-EDTA decomplexation.

For comprehending the influence of temperature, the degradation of Cu(II)-EDTA during CEC in the temperature range of 25 to 55 °C was surveyed. Fig. 2f revealed the best degradation effect at 35 °C. On the one hand, elevating the temperature would strengthen the activity of free radicals, on the other hand, when the temperature rose, the molecular activity of water intensified with the increase of molecular friction, so that the energy loss in the process of ultrasonic propagation was greater. In addition, when the temperature went up to a certain degree, the FEP powder would undergo a glass transition [35], which affects the CEC process. However, the effects of temperature may be complex and require to be further studied.

To evaluate the pH compatibility of CEC process, the decomplexation of Cu(II)-EDTA at various pH was compared. It was evident that Cu(II)-EDTA degraded 62.5 % at pH 2.0 for 150 min, and reached 86.4 % at pH 4.0, and it was reduced to 49.9 %, 13.6 % and 9.1 % at the solution pH 6.0, 8.0 and 10.0, respectively (Fig. 2g). It was clear that the decomplexation of Cu(II)-EDTA was suppressed to some extent not only under alkaline conditions, but also under superacid conditions, which was consistent with the calculation results of kinetic constants (Fig. 2h). We mentioned that the degradation of organic pollutants in CEC was achieved by the occurrence of ROS formed by electron transfer, but hydrogen ion adsorption would compete with electron transfer. The excessive presence of hydrogen ions in the system leads to their adsorption onto the surface of the dielectric powder [36], which inhibited the electron transfer between the water molecules and the dielectric powder. Other studies have also reported that the degradation of Cu(II)-EDTA was facilitated in acidic environment, whereas alkaline conditions impeded the process [37,38]. The hydrolysis forms of Cu(II)-EDTA were rested with the pH condition. The main species in the solution were CuH_2EDTA and $CuHEDTA^-$ at pH 2, and it was mainly $CuEDTA^{2-}$ and $CuHEDTA^-$ at pH 4, and $CuEDTA^{2-}$ was the only component at pH 6–10 [39]. In effect, protonated species CuH_2EDTA and $CuHEDTA^-$ were more easily oxidized by •OH radicals than deprotonated species $CuEDTA^{2-}$. In addition, the released copper ions are more likely to precipitate at high pH [40].

The degradation of Cu(II)-EDTA was surveyed at various molar ratios of copper and EDTA (1:1, 1:2, 1:4) with the view of being aware of the impact of superfluous EDTA. The decomplexation of Cu(II)-EDTA with molar ratio of 1:2 and 1:4 was significantly inhibited compared with the Cu complex with a molar ratio of 1:1 (Fig. 2i). The typical stoichiometry for the chelation of metal ions with EDTA is 1:1, and when present in excess, unbound EDTA will be free in solution [41]. Therefore, free EDTA would compete with Cu(II)-EDTA for the ROS, and impede the decomposition of Cu-EDTA.

3.3. Identification of reactive oxygen species

For the purpose of revealing the degradation mechanism of Cu(II)-EDTA, ROS generated in CEC was investigated systematically. The active materials were identified by EPR and free radical quenching agent, which confirmed the charge transfer and Cu(II)-EDTA degradation pathways. 100 mM DMPO was employed as a scavenger to capture •OH radicals produced during the catalytic reaction. Simultaneously containing 100 mM DMPO and 1 mM isopropyl alcohol (IPA) was used to trap $•O_2^-$ radicals, where the utilization of IPA was employed for the purpose of quenching •OH radicals, increasing the chance of DMPO trapping $•O_2^-$ radicals. As exhibited in Fig. S5, under ultrasonic stimulation, no signal was generated in the solution without FEP particles, while after FEP particles were added, the characteristic peaks of DMPO-•OH in the quadruple state (Fig. 3a) and DMPO-•OOH in the sextuple state were measured (Fig. 3b). The reason for this phenomenon is that H_2O in the solution undergoes oxidation by losing electrons, while O_2 undergoes reduction by gaining electrons. Additionally, due to the higher reactivity of •OH radicals with DMPO, the DMPO-•OOH peak predominantly appeared in a quadruple state. The generation of these two kinds of free radicals, •OH radicals and $•O_2^-$ radicals, exhibited continuous accumulation as ultrasound time was extended in Fig. 3c-d, indicating that FEP and water would generate •OH radicals and $•O_2^-$ radicals constantly under ultrasonic stimulation. Different concentrations (0.1 mM∼ 0.8 mM) of IPA and chloroform (Chlo) were added in the reaction to quench •OH radicals and $•O_2^-$ radicals (Fig. 3e-f), so as to examine the degradation of Cu(II)-EDTA by ROS attack. The EPR spectrum and the degradation effect of Cu(II)-EDTA after the addition of 4 mM IPA were depicted in Fig. S6-8. Above results showed that with the increasing concentration of free radical quencher, the decomplexation of Cu(II)-EDTA was getting worse and the signal of ROS was significantly weakened, which proved the important role of ROS during CEC process. Afterwards, 1 mM of $AgNO_3$ was introduced into the reaction system as an electron sacrificial agent to investigate whether the generation of free radicals attacking Cu(II)-EDTA through electron transfer. As demonstrated in Fig. S9, the addition of $AgNO_3$ in the reaction system resulted in a significant inhibition of Cu(II)-EDTA degradation. The comparison of H_2O_2 production with the addition of free radical quenchers and electron sacrificial agent under different ultrasonic time was shown in Fig.S10. On the whole, •OH radicals and $•O_2^-$ radicals generating in CEC process through electron transfer would attack Cu(II)-EDTA and realize the degradation of it.

3.4. Mechanism of producing ROS during CEC

The aforementioned findings and analysis serve as the foundation for the potential mechanism degradation of Cu(II)-EDTA during CEC, which could be divided into two processes: oxygen reduction and water oxidation (Fig. 4a). Water oxidation was the process by which water molecules interact with FEP particles, resulting in electron transfer to the surface of FEP particles and subsequent formation of water radical cations. These species would participate in subsequent reactions, such as protonation or deprotonation reactions, leading to the production of hydronium cations and •OH radicals [42]. At the same time, in oxygen reduction, the continuous generation and rupture of cavitation bubbles under ultrasonic environment resulted in the capture of electrons on the surface of FEP particles by O_2 [43]. This leaded to the formation of $•O_2^-$ radicals, which subsequently generated •OH radicals through a chain reaction [44]. The relative accumulation of •OH during the CEC reaction was shown in Fig. S11.

Water oxidation:

$$H_2O \rightarrow e^- + H_2O^{•+} \quad (1)$$

$$H_2O^{•+} \rightarrow \cdot OH + H^+ \quad (2)$$

Oxygen reduction:

$$O_2 + e^- \rightarrow \cdot O_2^- \quad (3)$$

$$\cdot O_2^- + H^+ \rightarrow \cdot OOH \quad (4)$$

$$\cdot OOH^- + H^+ + e^- \rightarrow H_2O_2 \quad (5)$$

$$H_2O_2 + e^- \rightarrow \cdot OH + OH^- \quad (6)$$

The ROS, which contain •OH and $•O_2^-$ radicals, ultimately reacted with Cu(II)-EDTA to achieve the degradation of it.

The energy barriers associated with these electron exchange processes were calculated and determined using Density Functional Theory (DFT), thereby investigating the impact of the ultrasound on electron transfer at the surface of dielectric powder. The specific calculation

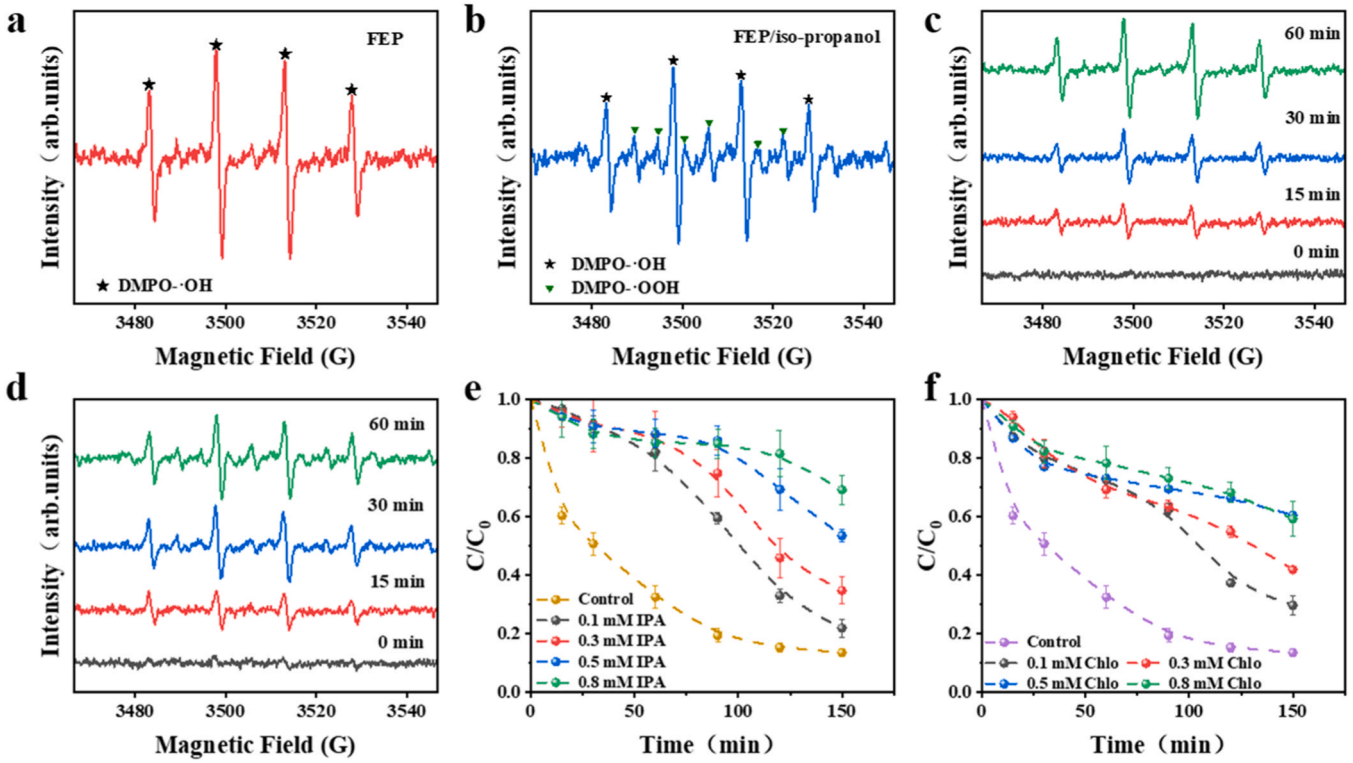

Fig. 3. EPR spectrums for (a) DMPO-·OH in the presence of FEP, (b) DMPO-·OOH in the presence of FEP/iso-propanol during ultrasonic captured by DMPO. Variation of EPR spectra for (c) DMPO-·OH, (d) DMPO-·OOH with reaction time. Comparison of Cu(II)-EDTA decomplexation with different quenching agent concentrations versus time of (e) iso-propanol, (f) chloroform.

details are available in Supporting Information. By simulating the high-pressure environment caused by bubble bursting, in both cases of H_2O/FEP and FEP* /O_2, the band gap between the lowest unoccupied molecular orbital (LUMO) and highest occupied molecular orbital (HOMO) gradually diminished as the system volume was compressed (Fig. S12). The calculation results indicated that the compression of volume to 70 % leaded to a reduction in the energy barriers of electron transfer by 4.43 % and 7.29 % (Fig. 4b), respectively. Consequently, in the CEC process, the high-pressure environment effectively diminished the energy barrier associated with electron transfer and facilitates its occurrence.

3.5. Decomplexation pathways of Cu(II)-EDTA and recovery of copper

To have more insights into the decomplexation of Cu(II)-EDTA, HPLC-MS was used to detect the characters of it in the catalytic reaction, thus deduced the degradation pathway of Cu(II)-EDTA and the evolution of its intermediate products. As shown in Fig. S13 and Fig. 5a, the main identified intermediates were Cu(II)-ED3A, Cu(II)-EDDA, Cu(II)-NTA, Cu(II)-IDA, IMDA, oxalic acid and glyoxylic acid. Meanwhile, with the extension of reaction time, the response peak area varied with the relative strength of the intermediates. This explained that the degradation of Cu(II)-EDTA coming true by •OH and $•O_2^-$ involved a continuous course of decarboxylation and deaminization. For investigating the function of deaminization and decarboxylation courses to the degradation process of Cu(II)-EDTA, the concentration of Cu(II)-EDTA and its intermediates was monitored during the CEC process, and the fractions of the intermediates among all intermediates at different time were subsequently computed. In Fig. 5b, the proportion of decarboxylated intermediates in the decomplexation process of Cu(II)-EDTA was prominently higher than deaminated intermediates, which was attributed to the lower energy barrier of ROS radicals facilitated decarboxylated reaction compared with deaminization reaction [45]. Other trace amounts of degradation products were also detected in HPLC-MS (Fig. S14), which ascribed to the fact that the degradation of Cu(II)-EDTA was a complex reaction process and need to be further researched. Above consequences manifested that the amino group of Cu(II)-EDTA was attacked selectively by ROS for decarboxylation and deaminization, in which decarboxylation was dominant, giving rise to efficient transformation of complex Cu to disengaged Cu^{2+}. Fig. 5a further presented the main degradation pathways of Cu(II)-EDTA during CEC. It demonstrated that decarboxylation and deaminization could be realized through the attack of ROS in the CEC process, promoting the continuous breaking of Cu-O and Cu-N bonds in Cu(II)-EDTA. In the degradation of Cu(II)-EDTA, the intermediate products underwent continuous oxidation and decomposition due to the relentless attack of ROS, ultimately leading to mineralization. The ongoing decomposition and potential mineralization of Cu(II)-EDTA would alleviate its acute toxicity [46,47].

Commercial CuSe was used as the cathode electrode in CDI with the view of implementing the recovery of free Cu^{2+} in solution. The specific experimental device was shown in Fig. S15. In our previous studies, it has been confirmed that CuSe as a cathode electrode in CDI could undergo redox reaction with Cu^{2+} in solution to produce Cu_2Se during electroadsorption [48], and achieved efficient selective adsorption of Cu^{2+}. Fig. 5c illustrated that the recovery rate of Cu in Cu(II)-EDTA after degradation during CEC process was significantly higher than without CEC treatment, which indicated the importance of decomplexation in the treatment of metal complexes. Meanwhile, the recovery effect of Cu was continuously enhanced with the raising of voltage (Fig. 5d), which certified that the reaction parameters could be sequentially optimized and further amplified [49].

3.6. Applicability analysis of CEC

The applicability of CEC process to degrade other heavy metal

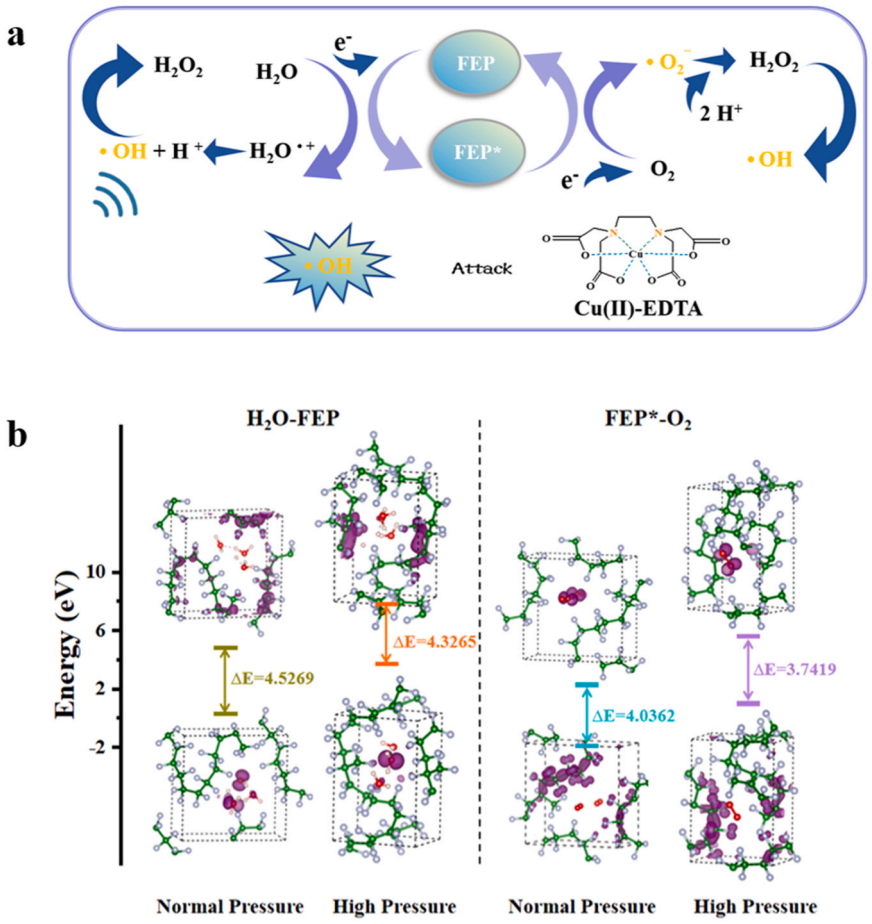

Fig. 4. (a) Proposed reaction mechanism for the degradation of Cu(II)-EDTA in CEC course. (b) DFT calculations and assessment of energy barrier between LUMO and HOMO for H_2O/FEP and FEP* /O_2 in different cases.

complexes was further assessed. Fig. 6a-c demonstrated Pb(II)-EDTA, Cd (II)-EDTA, and Ni(II)-EDTA could be effectively degraded during CEC process. Although the reaction parameters need to be further optimized due to the different complexation forms of different heavy metal complexes, this well proved the universal applicability of CEC for decomplexation of heavy metal complexes, revealing that CEC process had excellent application potential in degrading metal complexes and releasing metal ions. As depicted in Fig. 6d-e, the degradation ratio of Cu (II)-EDTA remained consistent with the initial effect after 4 cycles, with the kinetic constant keeping stable, indicating excellent stability and durability. In the specific recycling process, FEP could be effectively recovered after simple filtration, washing and drying, and the recovered powder showed no significant alterations in appearance, color, aggregation state (Fig. S16), thereby demonstrating its excellent recycling stability and economic viability.

CEC phenomenon is common and polymer materials that can be used as dielectric powder are inexpensive and effortless to obtain [50]. Simultaneously, CEC has obvious advantages compared with other metal complex treatment technologies (Table S1). Therefore, based on the principle of CEC, an economical wastewater treatment system for heavy metal complexs was designed, as shown in Fig. 6f. At the same time, we expect that this innovative strategy has excellent applications in organic pollutant wastewater treatment, heavy metal resource recovery, active substance research and other related fields.

4. Conclusion

The discharge of metal-organic complexes, which are commonly found contaminants in industrial organic wastewater, is substantial. Given the prominent pollution caused by metal complexes and resources depletion, it is imperative to achieve effective treatment of these complexes and facilitate the recovery of valuable metals. In this research, a promising technique for coupling contact-electro-catalysis with electroadsorption had been demonstrated to destroy Cu(II)-EDTA and capture Cu^{2+}. In this treatment process, contact of FEP particles with water would generate hydroxyl radicals and superoxide radicals under ultrasonic to realize the decarboxylation and deaminization of Cu (II)-EDTA, and promote the break of Cu-O and Cu-N bonds. By investigating the degradation pathway of Cu(II)-EDTA and the evolution of its intermediates, it has been confirmed that decarboxylation predominantly governs the degradation process of Cu(II)-EDTA in CEC. Subsequently, the released Cu^{2+} were adsorbed by the CuSe electrode in the electroadsorption, which realized the effective recovery of Cu. Impressively, this strategy had satisfactory applicability to other metal combinations and excellent cycle stability, and the catalytic efficiency could be further improved by increasing the number of electron transfers through parameter optimization. In the future, we can employ the mechanical energy widely existing in nature, such as wind energy and hydrodynamic energy, as a green energy to drive catalytic reactions to achieve environmentally friendly metal complex degradation and metal recycling.

Environmental implications

The heavy metal complexes which were more stable, toxic and diffusible pose challenges for their removal through conventional treatment methods, bringing about significant risks to aquatic ecosystems. The current treatment methods for metal complexes typically

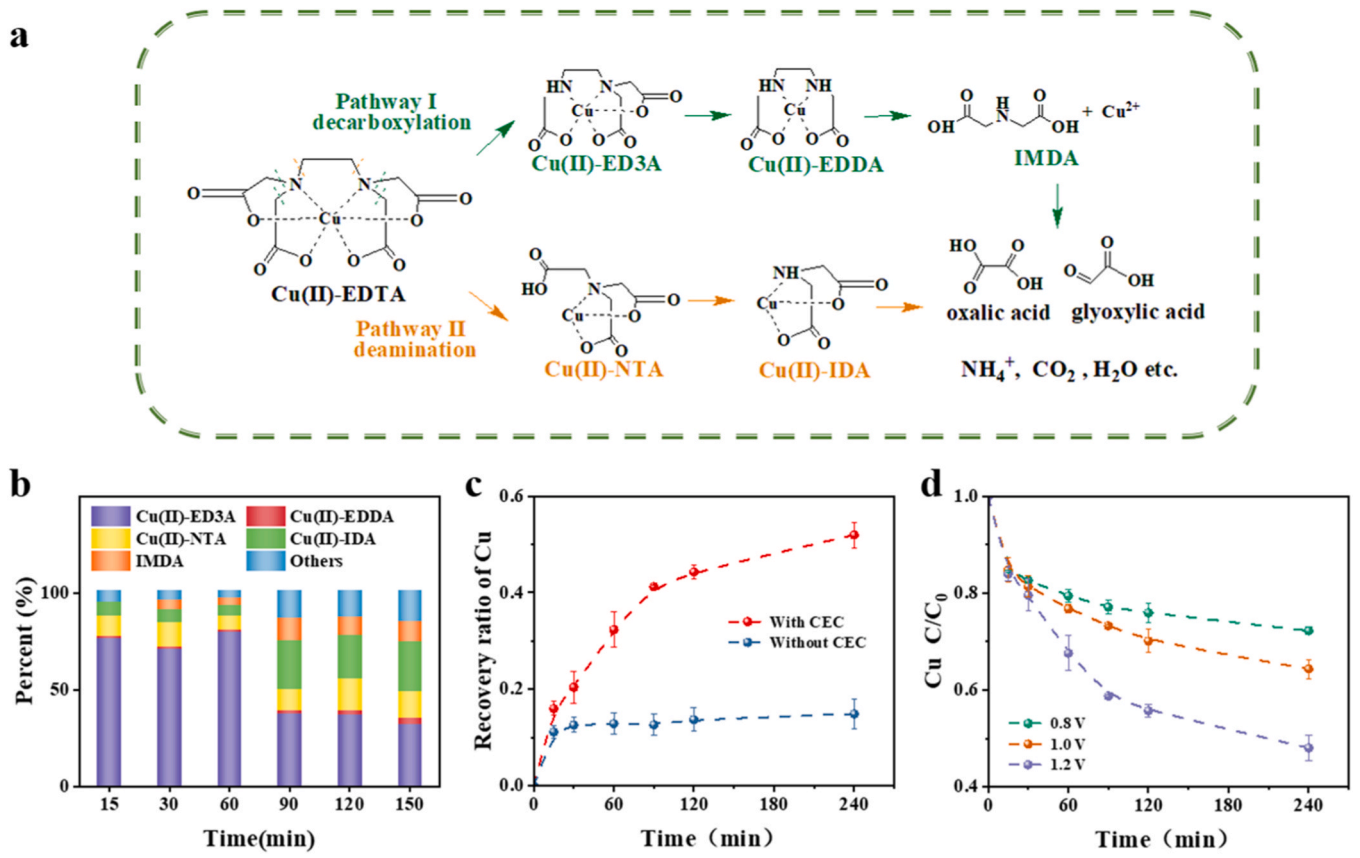

Fig. 5. (a) Major degradation pathways of Cu(II)-EDTA during CEC. (b) Comparison of the proportion of intermediates at different time during CEC reaction. (c) The influence of CEC reaction on the recovery of Cu. (d) Plots of Cu removal of the CuSe electrode versus time at different potentials.

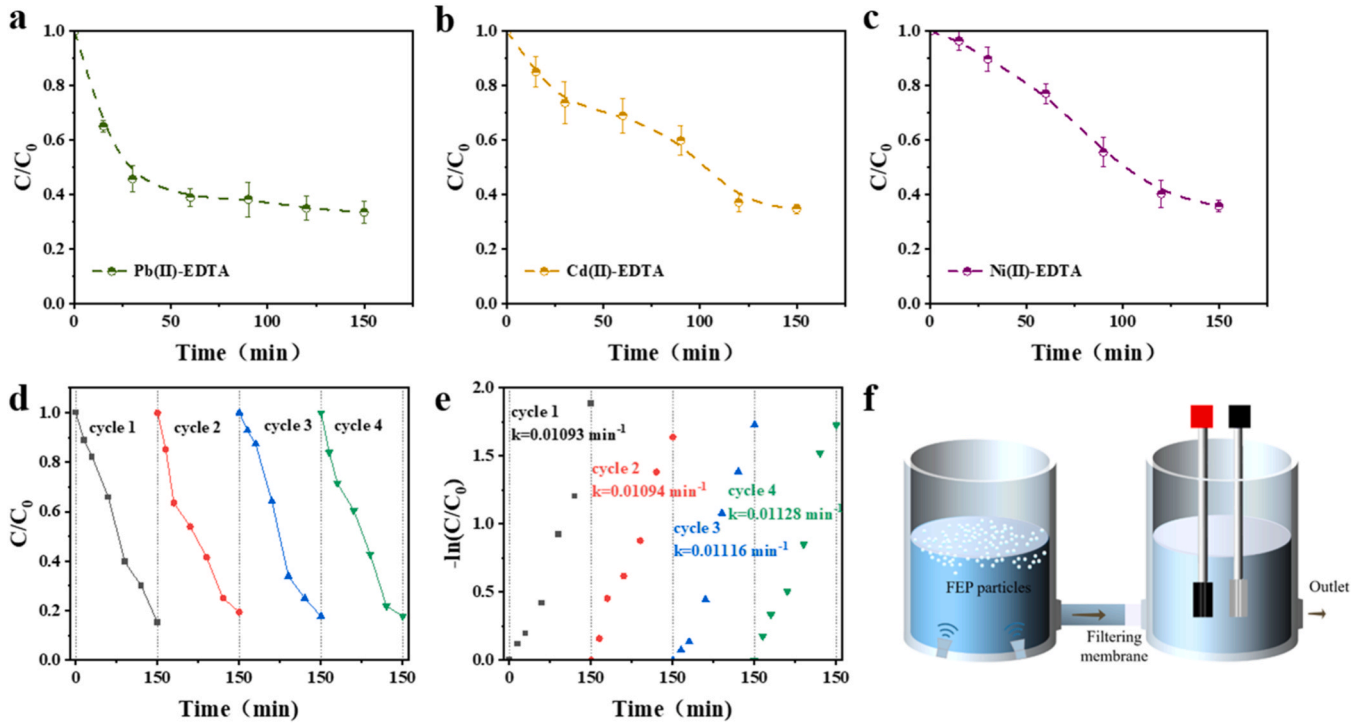

Fig. 6. Decomplexation of metal-EDTA complexes during CEC [(a) Pb(II)-EDTA, (b) Cd(II)-EDTA, (c) Ni(II)-EDTA]. (d) Cycle performance of Cu(II)-EDTA removal with FEP particles during CEC. (e) Change curve of $-\ln(C/C_0)$ with time for different cycles. (f) Expected large application of CEC coupled with CDI for the treatment and recovery of metal-organic pollutant.

involve the utilization of oxidizing agents and supplementary precipitation. In this research, a promising innovation technique for coupling contact-electro-catalysis with CDI was demonstrated to degrade Cu(II)-EDTA and capture Cu^{2+} synchronously without the requirement of oxidants or precipitants. The proposed strategy represents a pioneering catalytic pathway that offers an expanded range of materials and enhanced electrification benefits, showing excellent application potential.

CRediT authorship contribution statement

Lin Zhao: Visualization. **Shiyong Wang:** Writing – review & editing, Data curation, Conceptualization. **Xiaoyan Shen:** Writing – review & editing, Validation, Investigation, Formal analysis, Data curation. **Haoran Song:** Resources. **Wei Li:** Resources. **Changping Li:** Resources. **Gang Wang:** Supervision, Resources, Conceptualization. **Sihao Lv:** Resources.

Declaration of Competing Interest

The authors declare that they have no known competing financial interests or personal relationships that could have appeared to influence the work reported in this paper.

Data availability

No data was used for the research described in the article.

Acknowledgements

The authors acknowledge financial support from the National Natural Science Foundation of China (Nos. 22178055, 21878049); and Dongguan Introduction Program of Leading Innovative and Entrepreneurial Talents. The authors acknowledge the support of characterization from Dongguan University of Technology Analytical and Testing Center.

Appendix A. Supporting information

Supplementary data associated with this article can be found in the online version at doi:10.1016/j.jhazmat.2024.134548.

References

[1] Sahebjamee, N., Soltanieh, M., Mousavi, S.M., Heydarinasab, A., 2019. Removal of Cu^{2+}, Cd^{2+} and Ni^{2+} ions from aqueous solution using a novel chitosan/polyvinyl alcohol adsorptive membrane. Carbohydr Polym 210, 264–273.
[2] Fu, F., Wang, Q., 2011. Removal of heavy metal ions from wastewaters: a review. J Environ Manag 92, 407–418.
[3] Huang, X., Wang, X., Guan, D.-X., Zhou, H., Bei, K., Zheng, X., et al., 2019. Decomplexation of Cr(III)-EDTA and simultaneous abatement of total Cr by photo-oxidation: efficiency and in situ reduction of intermediate Cr(VI). Environ Sci Pollut R 26, 8516–8524.
[4] Huang, X., Wang, Y., Li, X., Guan, D., Li, Y., Zheng, X., et al., 2019. Autocatalytic decomplexation of Cu(II)-EDTA and simultaneous removal of aqueous Cu(II) by UV/chlorine. Environ Sci Technol 53, 2036–2044.
[5] Zou, X., Zhang, Y., Wei, K., Dai, J., Mao, C., Hu, L., et al., 2023. One-stop rapid decomplexation and copper capture of Cu(II)-EDTA with nanoscale zero valent iron. J Hazard Mater 446, 130752.
[6] Liu, Y., Feng, Y., Zhang, Y., Mao, S., Wu, D., Chu, H., 2019. Highly efficient degradation of dimethyl phthalate from Cu(II) and dimethyl phthalate wastewater by EDTA enhanced ozonation: performance, intermediates and mechanism. J Hazard Mater 366, 378–385.
[7] Xu, Z., Zhang, Q., Li, X., Huang, X., 2022. A critical review on chemical analysis of heavy metal complexes in water/wastewater and the mechanism of treatment methods. Chem Eng J 429, 131688.
[8] Li, J., Ma, J., Dai, R., Wang, X., Chen, M., Waite, T.D., et al., 2020. Self-enhanced decomplexation of Cu-organic complexes and Cu recovery from wastewaters using an electrochemical membrane filtration system. Environ Sci Technol 55, 655–664.
[9] Zhao, X., Guo, L., Hu, C., Liu, H., Qu, J., 2014. Simultaneous destruction of Nickel (II)-EDTA with TiO_2/Ti film anode and electrodeposition of nickel ions on the cathode. Appl Catal B 144, 478–485.
[10] Zhao, X., Guo, L., Zhang, B., Liu, H., Qu, J., 2013. Photoelectrocatalytic oxidation of Cu(II)-EDTA at the TiO_2 electrode and simultaneous recovery of Cu(II) by electrodeposition. Environ Sci Technol 47, 4480–4488.
[11] Yu, J., Deng, W., Huang, X., Zhao, M., Li, X., Zhang, T., et al., 2024. Intramolecular generation of endogenous Cu(III) for selectively self-catalytic degradation of Cu (II)-EDTA from wastewater by UV/peroxymonosulfate. J Hazard Mater 465, 133521.
[12] Chen, C., Liu, P., Li, Y., Tian, H., Zhang, Y., Zheng, X., et al., 2022. Electro-peroxone enables efficient Cr removal and recovery from Cr(III) complexes and inhibits intermediate Cr(VI) generation in wastewater: performance and mechanism. Water Res 218, 118502.
[13] Xu, Z., Shan, C., Xie, B., Liu, Y., Pan, B., 2017. Decomplexation of Cu(II)-EDTA by UV/persulfate and UV/H_2O_2: efficiency and mechanism. Appl Catal B 200, 439–447.
[14] Wang, Q., Zhang, Y., Li, Y., Ren, J., Qu, G., Wang, T., et al., 2022. Simultaneous Cu-EDTA oxidation decomplexation and Cr(VI) reduction in water by persulfate/formate system: reaction process and mechanisms. Chem Eng J 427, 131584.
[15] Zhang, L., Wu, B., Zhang, G., Gan, Y., Zhang, S., 2019. Enhanced decomplexation of Cu(II)-EDTA: the role of acetylacetone in Cu-mediated photo-Fenton reactions. Chem Eng J 358, 1218–1226.
[16] He, S., Li, T., Zhang, L., Zhang, X., Liu, Z., Zhang, Y., et al., 2021. Highly effective photocatalytic decomplexation of Cu-EDTA by MIL-53(Fe): highlight the important roles of Fe. Chem Eng J 424, 130515.
[17] Lee, S.S., Bai, H., Liu, Z., Sun, D.D., 2015. Green approach for photocatalytic Cu (II)-EDTA degradation over TiO_2: toward environmental sustainability. Environ Sci Technol 49, 2541–2548.
[18] Thalmann, B., Gunten, Uv, Kaegi, R., 2018. Ozonation of municipal wastewater effluent containing metal sulfides and metal complexes: kinetics and mechanisms. Water Res 134, 170–180.
[19] Chen, C., Chen, A., Huang, X., Ju, R., Li, X., Wang, J., et al., 2021. Enhanced ozonation of Cu(II)-organic complexes and simultaneous recovery of aqueous Cu (II) by cathodic reduction. J Clean Prod 298, 126837.
[20] Liu, B., Pan, S., Liu, Z., Li, X., Zhang, X., Xu, Y., et al., 2020. Efficient removal of Cu (II) organic complexes by polymer-supported, nanosized, and hydrated Fe(III) oxides through a Fenton-like process. J Hazard Mater 386, 121969.
[21] Fu, F., Xie, L., Tang, B., Wang, Q., Jiang, S., 2012. Application of a novel strategy—Advanced Fenton-chemical precipitation to the treatment of strong stability chelated heavy metal containing wastewater. Chem Eng J 189-190, 283–287.
[22] Huang, X., Xu, Y., Shan, C., Li, X., Zhang, W., Pan, B., 2016. Coupled Cu(II)-EDTA degradation and Cu(II) removal from acidic wastewater by ozonation: performance, products and pathways. Chem Eng J 299, 23–29.
[23] Liu, Y., Lu, M., Yin, Y., Zhou, J., Qu, G., Zhang, Y., et al., 2022. Self-catalytic Fenton-like reactions stimulated synergistic Cu-EDTA decomplexation and Cu recovery by glow plasma electrolysis. Chem Eng J 433, 134601.
[24] Sun, Y., Zhang, C., Rong, H., Wu, L., Lian, B., Wang, Y., et al., 2022. Electrochemical Ni-EDTA degradation and Ni removal from electroless plating wastewaters using an innovative Ni-doped PbO_2 anode: optimization and mechanism. J Hazard Mater 424, 127655.
[25] Song, W., Zhang, M., Qiu, H., Li, C., Chen, T., Jiang, L., et al., 2022. Insulator polymers achieve efficient catalysis under visible light due to contact electrification. Water Res 226, 119242.
[26] Zhao, X., Su, Y., Berbille, A., Wang, Z., Tang, W., 2023. Degradation of methyl orange by dielectric films based on contact-electro-catalysis. Nanoscale 15, 6243–6251.
[27] Wang, Z., Berbille, A., Feng, Y., Li, S., Zhu, L., Tang, W., et al., 2022. Contact-electro-catalysis for the degradation of organic pollutants using pristine dielectric powders. Nat Commun 13, 130.
[28] Chen, Z., Lu, Y., Liu, X., Li, J., Liu, Q., 2023. Novel magnetic catalysts for organic pollutant degradation via contact electro-catalysis. Nano Energy 108, 108198.
[29] Xu, Y., Xiang, S., Zhang, X., Zhou, H., Zhang, H., 2022. High-performance pseudocapacitive removal of cadmium via synergistic valence conversion in perovskite-type $FeMnO_3$. J Hazard Mater 439, 129575.
[30] Yang, X., Liu, L., Tan, W., Qiu, G., Liu, F., 2018. High-performance Cu^{2+} adsorption of birnessite using electrochemically controlled redox reactions. J Hazard Mater 354, 107–115.
[31] Mamaril, G.S.S., de Luna, M.D.G., Bindumadhavan, K., Ong, D.C., Pimentel, J.A.I., Doong, R.-A., 2021. Nitrogen and fluorine co-doped 3-dimensional reduced graphene oxide architectures as high-performance electrode material for capacitive deionization of copper ions. Sep Purif Technol 272, 117559.
[32] Nie, L., Wang, L., Wang, X., He, M., Wang, J., Lv, Y., et al., 2024. Enhancing copper recycling through synergistic valence conversions in MnOx-modified capacitive deionization electrodes. Chem Eng J 485, 149960.
[33] Berbille, A., Li, X.F., Su, Y., Li, S., Zhao, X., Zhu, L., et al., 2023. Mechanism for generating H_2O_2 at water-solid interface by contact-electrification. Adv Mater 35, 2304387.
[34] Zhao, J., Zhang, X., Xu, J., Tang, W., Wang, Z., Fan, F., 2023. Contact-electro-catalysis for direct synthesis of H_2O_2 under ambient conditions. Angew Chem, Int Ed 135, 1–8.
[35] Dong, X., Wang, Z., Berbille, A., Zhao, X., Tang, W., Wang, Z., 2022. Investigations on the contact-electro-catalysis under various ultrasonic conditions and using different electrification particles. Nano Energy 99, 107346.
[36] Nie, J., Ren, Z., Xu, L., Lin, S., Zhan, F., Chen, X., et al., 2019. Probing contact-electrification-induced electron and ion transfers at a liquid–solid interface. Adv Mater 32, 1905696.

[37] Zeng, H., Tian, S., Liu, H., Chai, B., Zhao, X., 2016. Photo-assisted electrolytic decomplexation of Cu-EDTA and Cu recovery enhanced by H_2O_2 and electro-generated active chlorine. Chem Eng J 301, 371–379.
[38] Guan, W., Zhang, B., Tian, S., Zhao, X., 2018. The synergism between electro-Fenton and electrocoagulation process to remove Cu-EDTA. Appl Catal, B 227, 252–257.
[39] Wang, Q., Li, Y., Liu, Y., Ren, J., Zhang, Y., Qu, G., et al., 2021. Effective removal of the heavy metal-organic complex Cu-EDTA from water by catalytic persulfate oxidation: performance and mechanisms. J Clean Prod 314, 128119.
[40] Zu, D., Song, H., Li, C., Wang, Y., Du, R., Zhou, R., et al., 2022. Understanding the self-catalyzed decomplexation mechanism of Cu-EDTA in $Ti_3C_2T_x$ MXene/peroxymonosulfate process. Appl Catal, B 306, 121131.
[41] Wang, T., Cao, Y., Qu, G., Sun, Q., Xia, T., Guo, X., et al., 2018. Novel Cu(II)-EDTA decomplexation by discharge plasma oxidation and coupled Cu removal by alkaline precipitation: underneath mechanisms. Environ Sci Technol 52, 7884–7891.
[42] Ma, J., Wang, F., Mostafavi, M., 2018. Ultrafast chemistry of water radical cation, $H_2O^{\bullet+}$, in aqueous solutions. Molecules 23, 244.
[43] Siahrostami, S., Villegas, S.J., Bagherzadeh Mostaghimi, A.H., Back, S., Farimani, A.B., Wang, H., et al., 2020. A review on challenges and successes in atomic-scale design of catalysts for electrochemical synthesis of hydrogen peroxide. ACS Catal 10, 7495–7511.
[44] Hayyan, M., Hashim, M.A., AlNashef, I.M., 2016. Superoxide ion: generation and chemical implications. Chem Rev 116, 3029–3085.
[45] Chen, Y., Mu, Y., Tian, L., Zheng, L., Mei, Y., Xing, Q., et al., 2023. Targeted decomplexation of metal complexes for efficient metal recovery by ozone/percarbonate. Environ Sci Technol 57, 5034–5045.
[46] Wang, Q., Yu, J., Chen, X., Du, D., Wu, R., Qu, G., et al., 2019. Non-thermal plasma oxidation of Cu(II)-EDTA and simultaneous Cu(II) elimination by chemical precipitation. J Environ Manag 248, 109237.
[47] Liu, Y., Wang, D., Xue, M., Song, R., Zhang, Y., Qu, G., et al., 2021. High-efficient decomplexation of Cu-EDTA and Cu removal by high-frequency non-thermal plasma oxidation/alkaline precipitation. Sep Purif Technol 257, 117885.
[48] Wang, S., Zhuang, H., Shen, X., Zhao, L., Pan, Z., Liu, L., et al., 2023. Copper removal and recovery from electroplating effluent with wide pH ranges through hybrid capacitive deionization using CuSe electrode. J Hazard Mater 457, 131785.
[49] Zhuang, H., Wang, S., Zhao, L., Pan, Z., Liu, L., Sillanpää, M., et al., 2022. Selective capture of Cu^{2+} using a redox-active cus cathode material in hybrid capacitive deionization. ACS EST Eng 2, 1722–1731.
[50] Wang, Y., Xu, Y., Dong, S., Wang, P., Chen, W., Lu, Z., et al., 2021. Ultrasonic activation of inert poly(tetrafluoroethylene) enables piezocatalytic generation of reactive oxygen species. Nat Commun 12, 3508.